Dyes and Pigments 120 (2015) 175–183

Contents lists available at ScienceDirect

Dyes and Pigments

journal homepage: www.elsevier.com/locate/dyepig

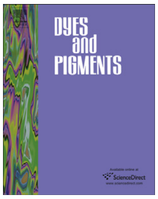

Self-assembly of a series of thiocyanate complexes with high two-photon absorbing active in near-IR range and bioimaging applications

Dandan Li, Qiong Zhang, Xuchun Wang, Shengli Li, Hongping Zhou, Jieying Wu, Yupeng Tian*

Department of Chemistry, Key Laboratory of Functional Inorganic Materials Chemistry of Anhui Province, Anhui University, Hefei 230039, PR China

A R T I C L E I N F O

Article history:
Received 2 January 2015
Received in revised form
14 March 2015
Accepted 17 March 2015
Available online 16 April 2015

Keywords:
Two-photon absorption
2 PA cross-sections
Near-infrared
Hetero-metal
Structure–property
Cell imaging

A B S T R A C T

A series of novel complexes bearing high fluorescence quantum yields and showing the peak two-photon absorption (2 PA) cross-sections in the near-infrared region, **$Zn(SCN)_2L_2$ (1)**, **$[Cd(SCN)_2L_2]_n$ (2)**, **$Co(SCN)_2L_4$ (3)**, **$Ni(SCN)_2L_4$ (4)**, **$[CdHgL_2(SCN)_4]_n$ (5)** and **$[MnHg(SCN)_4L_2]_n$ (6)**, containing functional chromophore (**L** = (E)-(4-diethyl anilinostyryl)pyridine), were synthesized in high yields. Crystal structures of all the complexes were confirmed. Hetero-metal complexes (**5**, **6**: L:M = 1:1) present much higher two-photon absorption (2 PA) cross-sections (σ) in comparison with those of the homo-metal complexes (L:M = 4:1 in **3** and **4**, L:M = 2:1 in **1** and **2**) and the free ligand (**L**) which may due to the fact that the hetero-metal complexes have more bridged anions (SCN^-), conjugated subunits $-[Hg(SCN)_2M]-$ and $-[Hg_2(SCN)_4M_2]-$. In addition, the results revealed that 2 PA response was much enhanced for the **$Zn(SCN)_2L_2$** and two-photon fluorescence cell imaging experiment proved its potential application.

1. Introduction

The research for functionalized materials with large molecular 2 PA cross sections (σ) has mushroomed because of their potential applications in two-photon excitation fluorescence microscopy [1–8], microfabrication [9,10], laser up-conversion [11–15], optical power limiting [16–18], three-dimensional (3D) fluorescence imaging [19–21], optical data storage [22–25], photodynamic therapy [26,27], two-photon fluorescent probe, and so on. Among these applications, bioimaging as two-photon fluorescence probes in living cells has recently been received much attention [28–30] due to the fact that among various conventional bio-imaging techniques, two-photon excitation microscopy is a highly sensitive and noninvasive tool particularly for living cell and tissue imaging. Since the 2 PA process is quadratic intensity dependent, the excitation in a two-photon excitation microscope is focused to a small volume in the focal plane where only in this volume there is sufficient laser intensity to generate appreciable excitation. The low photon flux outside the volume gives a negligible amount of fluorescence signal. As a result, the two-photon excitation process offers optical sectioning (depth discrimination) capability and higher spatial resolution. The confined excitation can greatly reduce the photobleaching and photodamage of the specimen during bioimaging. Most biological samples are relatively transparent to near-infrared light which shows less scattering and thus the use of the low-energy infrared excitation source can improve the penetration depth in tissues and cells allowing deeper tissue imaging. Furthermore, a high signal-to-noise ratio (SNR) can be achieved as the excitation and emission wavelengths are widely separated. To realize these applications, many strategies have been reported for the design of various two-photon absorbing materials [4,31–33], Much of the impetus for this technological exploration was provided by the synthesis of new dyes in the mid-1990s, which are much more efficient in direct 2 PA than those commercially available [34]. To facilitate the design and synthesis of new and stronger responsive two-photon absorbing materials, one available way to take advantage of the superior qualities of both inorganic and organic materials is to combine them in the same compound [35–48]. The introduction of ligated metal centers into an organic π-delocalizable framework may result in intense charge-transfer

---

* Corresponding author. Tel.: +86 551 5108151; fax: +86 551 5107342.
E-mail address: yptian@ahu.edu.cn (Y. Tian).

http://dx.doi.org/10.1016/j.dyepig.2015.03.039
0143-7208/© 2015 Elsevier Ltd. All rights reserved.

transitions and enhanced nonlinear optical response. In the nonlinear optical (NLO) material fields, thiocyanate complexes can been optimized for NLO properties by a polarizable π system, the hard nitrogen and the soft sulfur coordination, low-lying π* orbitals and the metal-to-ligand charge-transfer (MLCT) transition [49,50]. However, few endeavor has been devoted to investigation of the 2 PA effect of the thiocyanate complexes and different d electron configurations of transition metal complexes [51]. For pyridyl ligands, highly delocalized and easily polarizable system, can bind to a wide range of transition metal ions, and have large asymmetry in electronic distribution caused by intramolecular donor–acceptor charge transfer while they coordinate to metal ions [52]. In the case of the same organic ligand and anion SCN^-, how to choose metal ions to improve two-photon absorption cross section effectively is a scientific challenge, which can make contribution to the design of two-photon active complexes. These characters are crucial to design organic-inorganic hybrid materials with large 2 PA cross-section (σ).

Based on the consideration above, we have strategically designed and synthesized a series of novel thiocyanate complexes with high two-photon absorbing using $M(SCN)_2$ (M = Zn(II), Cd(II), Hg(II), Ni(II), Co(II), and Mn(II)) and pyridine ligand(**L**) (shown in Fig. 1). The structure–property relationships of these complexes have been systematically investigated. Considering the terminal sulfur atoms are relevant to biological systems [53,54], we singled out **$Zn(SCN)_2L_2$** (**1**) for biological imaging application research.

2. Experiments

2.1. General procedure

All chemicals and solvents were dried and purified by the standard methods. Elemental analysis was performed on a Perkin–Elmer 240C elemental analyzer. IR spectra were recorded with a Nicolet FTIR Nexus 870 instrument in the range 4000–400 cm^{-1} by using KBr pellets. ^1H NMR spectra were performed on a Bruker av 500 MHz Ultrashield spectrometer and are reported as parts per million (ppm) from TMS (δ). The linear absorption spectra were measured on a SPECORD S600 spectrophotometer. The single-photon emission fluorescence (SPEF) spectra measurements were performed using a Hitachi F-7000 fluorescence spectrophotometer. The two-photon emission fluorescence (TPEF) spectra were measured at femtosecond laser pulse and Ti: sapphire system (680–1080 nm, 80 MHz, 140 fs) as the light source. The excitation wavelengths for the complexes are 700–900 nm.

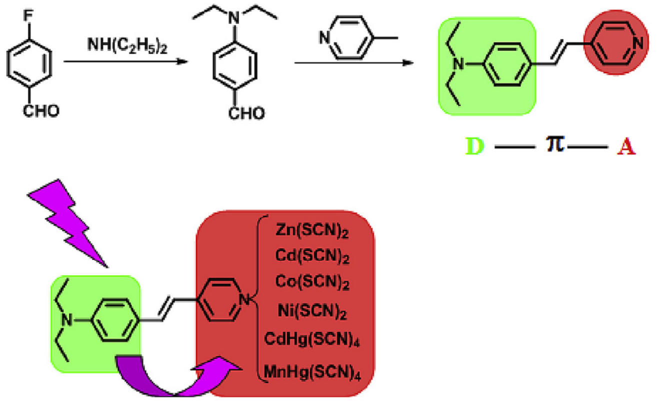

Fig. 1. Synthesis route of ligand.

2.2. Cell culture and incubation

HepG2 cells were seeded in 6 well plates at a density of 2 × 105 cells per well and grown for 96 h. For live cell imaging cell cultures were incubated with the chromophores (10% PBS: 90% cell media) at concentrations 40 μM and maintained at 37 °C in an atmosphere of 5% CO_2 and 95% air for incubation times ranging for 2 h. The cells were then washed with PBS (3 × 3 ml per well) and 3 ml of PBS was added to each well. The cells were imaged using confocal laser scanning microscopy and water immersion lenses.

2.3. Cell image

HepG2 cells were luminescently imaged on a Zeiss LSM 710 META upright confocal laser scanning microscope using magnification 40× and 100× water-dipping lenses for monolayer cultures. Image data acquisition and processing was performed using Zeiss LSM Image Browser, Zeiss LSM Image Expert and Image J.

2.4. Cytotoxicity assays in cells

To ascertain the cytotoxic effect of the compounds treatment over a 24 h period, the 5-dimethylthiazol-2-yl-2,5-diphenyl tetrazolium bromide (MTT) assay was performed. HepG2 cells were trypsinized and plated to ~70% confluence in 96-well plates 24 h before treatment. Prior to the compounds' treatment, the DMEM was removed and replaced with fresh DMEM, and aliquots of the compound stock solutions (500 μM DMSO) were added to obtain final concentrations of 1, 3, 5, 10, 20, 40, and 80 μM. The treated cells were incubated for 24 h at 37 °C and under 5% CO_2. Subsequently, the cells were treated with 5 mg/mL MTT (40 μL/well) and incubated for an additional 4 h (37 °C, 5% CO_2). Then, DMEM was removed, the formazan crystals were dissolved in DMSO (150 μL/well), and the absorbance at 490 nm was recorded. The cell viability (%) was calculated according to the following equation: cell viability % = OD_{490}(sample)/OD_{490}(control) × 100, where OD_{490}(sample) represents the optical density of the wells treated with various concentration of the compounds and OD_{490}(control) represents that of the wells treated with DMEM + 10% FCS. Three independent trials were conducted, and the averages and standard deviations are reported. The reported percent cell survival values are relative to untreated control cells.

2.5. Synthesis

The synthesis of the ligand and its complexes are shown in Supporting information.

2.6. Single-crystal structure analysis

Single-crystal measurements were carried out on a Bruker Smart 1000 CCD diffractometer equipped with a graphite crystal monochromator situated in the incident beam for data collection at room temperature. The determination of unit cell parameters and data collections were performed with M_o-K_α radiation (λ = 0.71073 Å). Unit cell dimensions were obtained with least-squares refinements, and all structures were solved by direct methods using SHELXL-97 [55]. The non-hydrogen atoms were located in successive difference Fourier syntheses. The final refinement was performed by full-matrix least-squares methods with anisotropic thermal parameters for non-hydrogen atoms on F^2. The hydrogen atoms were added theoretically and riding on the concerned atoms.

Crystallographic crystal data for complexes **1**–**6** are shown in Table S1. Selected bond lengths and bond angles are listed in